Sebastian Pech, René Richter and Jens Lienig

Non-occlusive pumping principle for blood pump application

Abstract:

Roller pumps are used in medicine to pump blood in extracorporeal blood circuits. Blood is subjected to mechanical stress in these peristaltic pumps, due to the complete tube occlusion. This stress causes damage to red blood cells (hemolysis). We present a novel peristaltic pumping principle that addresses these issues. In contrast to conventional roller pumps, the tube is stimulated by a circulating eccentric oscillation. Therefore, this type of pump does not require complete tube occlusion. The blood is less mechanically stressed and hemolysis is reduced by 55% compared to a roller pump.

Zusammenfassung:

In der Medizin werden Rollenpumpen zum Betreiben extrakorporaler Blutkreisläufe verwendet. Beim Einsatz dieser Verdrängerpumpen ist das Blut aufgrund der kompletten Schlauchquetschung (Okklusion) mechanischen Belastungen ausgesetzt. Dies führt zu einer Zerstörung der Erythrozyten (Hämolyse). Im Gegensatz zu konventionellen Rollenpumpen nutzt das vorgestellte neuartige Pumpprinzip eine umlaufene exzentrische Oszillation und verzichtet auf die vollständige Schlauchokklusion. Dadurch lässt sich die Hämolyse im Vergleich zu einer Rollenpumpe um 55% reduzieren.

Keywords: blood pump, hemolysis, peristaltic pump, red blood cell damage, tube occlusion

Schlagwörter: Blutpumpe, Hämolyse, Schlauchpumpe, Schlauchquetschung

1 Introduction

Extracorporeal blood pumps are used to operate extracorporeal life support systems (ECLS), dialysis or organ perfusion systems. Figure 1 shows the typical structure of an organ perfusion system with blood as the perfusion medium. This circuit is used to supply blood to organs (kidney, liver, lung, heart) outside the human body for transplantation or organ conditioning [1]. Blood is oxygenated in the circulation loop in a similar manner to a heart-lung machine and an ECLS. Depending on the organ, several blood pumps are required to perfuse different vascular systems.

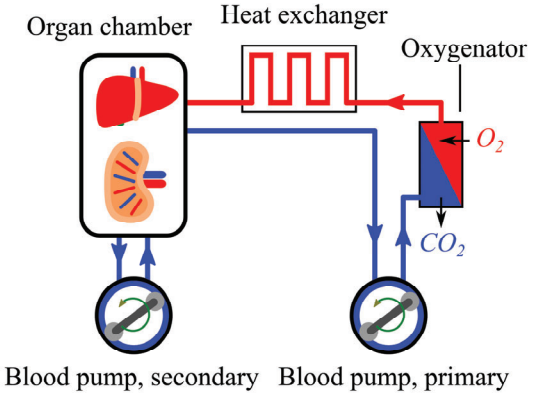

Fig. 1: Typical perfusion circulation system (according to [2]) to supply blood to organs outside the human body. Two roller pumps are used to perfuse the organ in this example.

1.1 Problem: red blood cell damage

Blood and its components are damaged during extracorporeal blood circulation and associated pumping. This is very taxing for a patient's organism and restricts the maximum permissible extracorporeal blood circulation time. In addi-

tion to the harmful impact of foreign surfaces, the shear stresses acting on the blood during the pumping process is the main cause of blood damage [3-5]. This shear stress leads to a deformation of the elastic cell membrane and results in mechanical destruction of the red blood cells – called hemolysis. Hemolysis caused by shear stress has already been investigated multiple times in the literature. Significant hemolysis is caused by shear stresses in the range τ = (80 – 400) Pa, according to [6, 7]. In addition to the magnitude, the duration of exposure to the shear stress is also critical. Mechanical hemolysis occurs at $\tau \geq 425$ Pa for a duration of 620 ms, according to [8].

1.2 State of the art: blood pumps

Depending on the application, roller pumps or centrifugal pumps are currently used to operate extracorporeal blood circuits. Roller pumps are often used for organ perfusion systems as they are easier to operate and the running costs are low. The method of operation and the blood damage mechanism of roller pumps are of special significance for the non-occlusive pumping principle presented in this article.
Roller pumps belong to the class of valveless positive displacement pumps. In contrast to conventional positive displacement pumps, a flexible tube forms the pump chamber (peristaltic pump). Two rollers occlude the tube completely and separate a partial volume of the tube. This volume is moved from the pump inlet to the pump outlet as a result of the periodic rotation of the rotor and the rollers (see Figure 2).

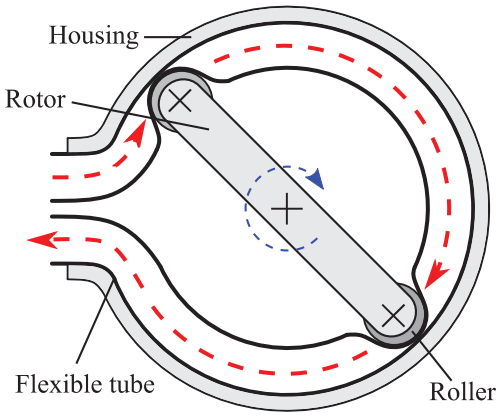

Fig. 2: Schematic illustration of a roller pump with volume flow (red) and rotor rotation (blue).

1.3 Red blood cell damage mechanism in roller pumps

Hemolysis caused by roller pumps is a function of the degree of occlusion, rotor speed, number of rollers, roller diameter, tube material, and inner tube diameter $d_{tube,i}$ [9-13]. Figure 3 shows the mass fraction of free hemoglobin *fHb* in blood plasma as an indicator of hemolysis. It is obvious that increasing occlusion or decreasing the remaining gap with w_{gap} causes increased hemolysis. In addition, hemolysis amplifies with smaller inner tube diameters $d_{tube,i}$ (Figure 3).
The contribution of this article is the introduction of a new pumping principle based on a peristaltic pump, which can be used to generate a volume flow without complete tube occlusion. This reduces the mechanical stress on the pumped fluid and decreases blood damage when used as a blood pump. This supports an increase in the maximum application duration combined with better therapeutic outcomes.

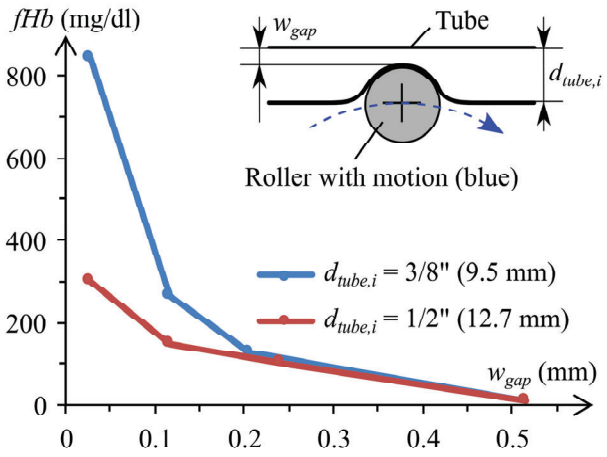

Fig. 3: Decrease in the mass fraction *fHb* of free plasma hemoglobin caused by hemolysis with an increase in the remaining gap w_{gap} for different inner tube diameters $d_{tube,i}$ at a flow Q = 4 l/min (according to [9]).

2 Pumping principle

2.1 Overview

In contrast to conventional roller pumps, the required mechanical energy is transferred into our pump tube by an oscillation. This oscillation causes a volume displacement and the propagation of a pulse wave in the pump tube. The volume flow Q_{out} is generated by a circulating eccentric oscillation arising from a rotationally symmetric pump design. As a result of the partial occlusion and the associated backflow Q_{back}, the non-occlusive pumping principle differs fundamentally from the principle of conventional peristaltic pumps. The main ideas behind our new pumping principle and its major components are described in the following four paragraphs.

2.2 Displacement and backflow

The operating principle of the non-occlusive peristaltic pump results from the superposition of a volume flow Q_{disp} generated by volume displacement and the backflow Q_{back}, which passes through the remaining gap of the partially occluded tube. An oscillation drives the pump. This oscillation is transmitted to a coupler and causes relative motion between the coupler and the tube. A portion of the fluid in the tube is displaced due to this relative motion. Consequently, a volume pulse propagates in the tube with velocity v_{disp}. Figure 4 shows the pump setup, the flows Q_{disp}, Q_{back}, Q_{out}, and the relative velocity v_{disp}.

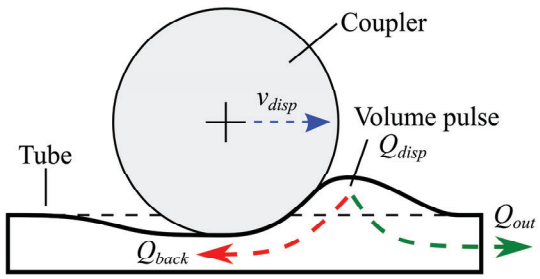

Fig. 4: Schematic illustration of the volume displacement in the non-occlusive pump with the relative velocity v_{disp} between the coupler and the tube (according to [2]).

2.3 Pulse wave propagation

In addition to the previously described volume pulse, a pulse wave is propagated in the tube by the circulating eccentric oscillation of the coupler. The pulse wave is propagated with velocity v_{pulse}. This specific propagation pace is the velocity at which pressure waves propagate within the tube system without forced excitation. The parameter v_{pulse} is comparable with a natural frequency (normal mode) of the tube system. Figure 5 shows the propagation of the pulse wave schematically.

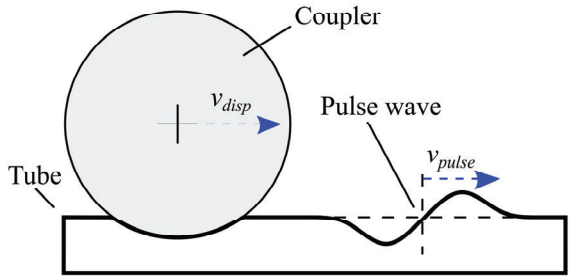

Fig. 5: Schematic illustration of the pulse wave propagation (velocity v_{pulse}) in the tube during the pumping operation (according to [2]).

2.4 Pump section

To implement the pumping principle the pump consists of a tube, a housing and a rotationally symmetrical coupler (see Figure 6A) [14-16]. In this pump section, the tube is placed in a gap between the coupler and the housing. The circulating eccentric oscillation is transmitted to the tube by the coupler. Consequently, the required volume pulse and the pulse wave are generated. Figure 6B shows the pump section projected onto developed surfaces for better understanding. The angle φ describes the coupler position with reference to the housing.

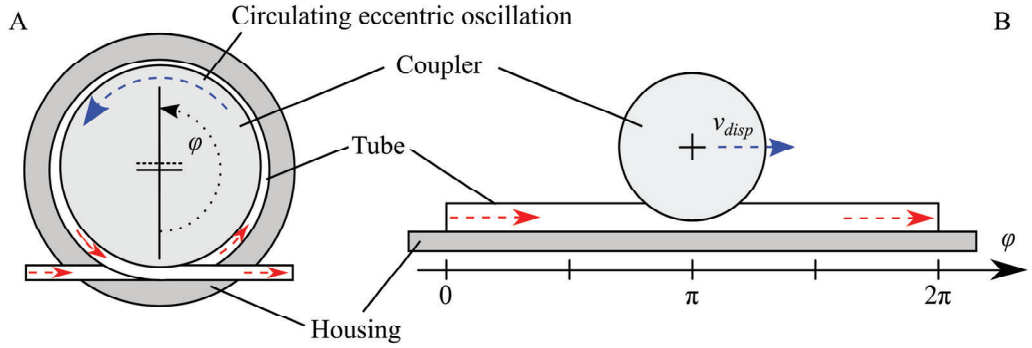

Fig. 6: Schematic illustration of the pump section: (A) top view showing the rotational symmetry, (B) unrolled surface view of rotational symmetry (according to [2]).

2.5 Decoupling

Finally, the fluid is decoupled from the tube winding. The flow Q_{out} is formed by superimposing Q_{disp} and Q_{back}, due to the non-occlusive pumping action. There is bidirectional flow at the pump outlet because of the circulating eccentric oscillation. To generate the desired unidirectional volume flow, a dynamic throttling device is installed that changes the flow resistance depending on the prevailing pressure in the tube. This is achieved by placing a dynamic flow resistor at the pump outlet, which acts passively on the tube. This resistor consists of a spring-mass oscillator that changes the tubular cross-section depending on the pressure prevailing in the tube. The volume flow Q_{out} is thus smoothed and rectified. Figure 7 illustrates the decoupling effect.

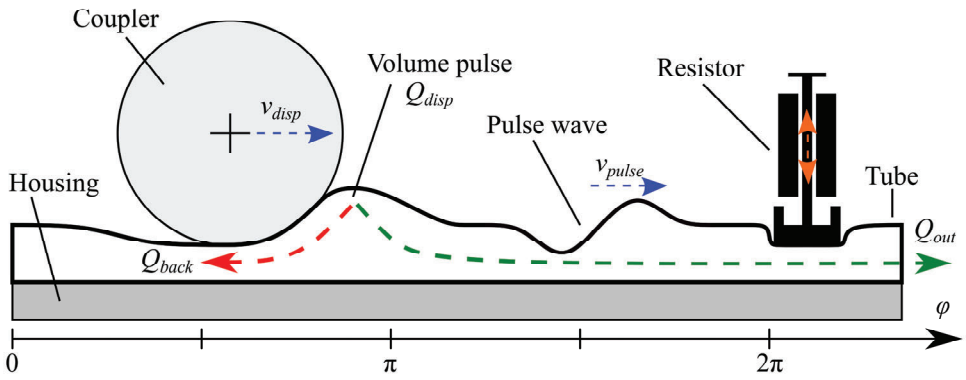

Fig. 7: Schematic illustration of the pumping principle with the decoupling process unrolled onto developed surfaces. As the pulse wave deflects (orange arrow) the resistor and expands the tube's cross-section, the volume pulse can pass with low losses.

The pump section forms an oscillator circuit due to the rotationally symmetrical design, the circulating eccentric oscillation of the coupler, and the resistor at the end of the tube winding. The pulse wave is ahead of the volume pulse when $v_{pulse} > v_{disp}$. This causes the pressure pulse of the pulse wave to deflect the resistor (see orange arrow in Figure 7). This in turn leads to an expansion in the tubular cross-section allowing the displaced volume to pass through the resistor with low losses. When the displaced volume has passed the point of restriction (i.e., the flow resistor), a low pressure regime is established in the pump tube. The tubular cross-section is thereby reduced by the resistor, which prevents the volume already pumped from flowing back.

3 Pump actuator

The circulating eccentric oscillation is generated by a radially symmetrical oscillating armature motor. Figure 8A shows the actuator design in longitudinal section. The actuator is driven by an electromagnetic transducer. Figure 8B illustrates the transducer in a cross-sectional view. It consists of a stator with multiple coils and an oscillating armature in the center. The oscillating armature is attached to a bending rod. A phase-shifted current applied to the stator coils produces armature motion causing a circulatory eccentric oscillation. This oscillation is transmitted by the bending rod to the coupler producing the described pumping action. The pump is controlled by the amplitude r_{osc} and the frequency f of the circulating eccentric oscillation.

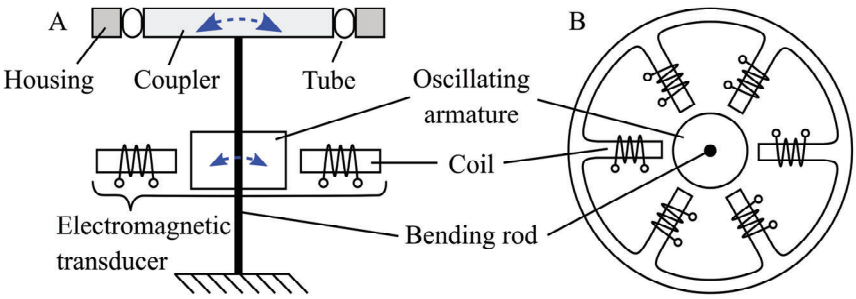

Fig. 8: Schematic illustration of the actuator to operate the pump (according to [14], [17]): (A) longitudinal section of the actuator, (B) cross-section of the electromagnetic transducer.

Figure 9 shows the pump section with the described components.

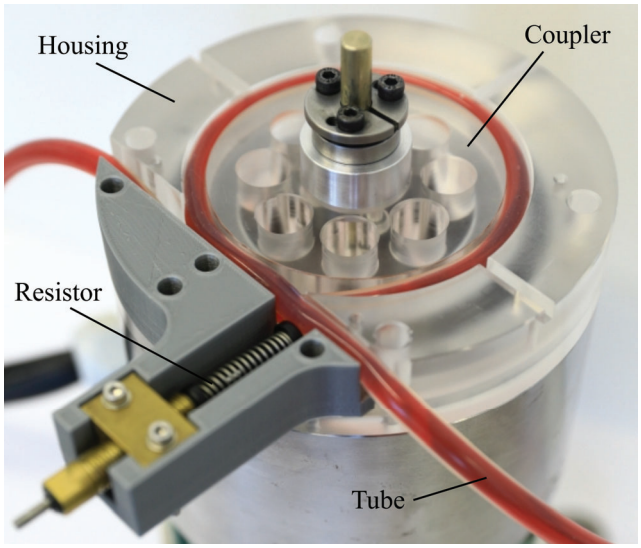

Fig. 9: Top view of the pump section of the non-occlusive peristaltic pump with the described components.

4 Pump simulation

4.1 Overview

Figure 10 shows the complete simulation model used to dimension a pump working according to the principle described above. The model consists of the first two submodels: 1) multibody simulation (MBS), 2) finite element analysis (FEA) and 3) hydraulic model.

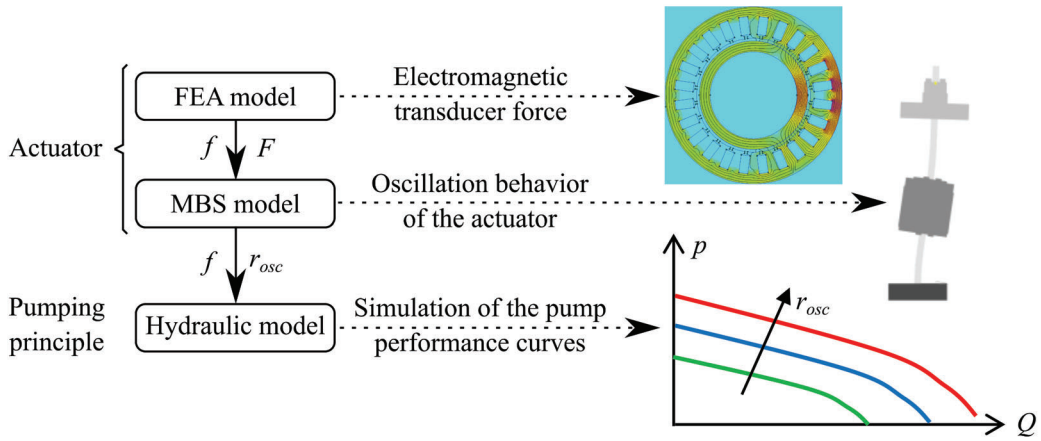

Fig. 10: Modelling structure for simulating the force generated by the electromagnetic transducer, the actuator oscillation behavior and the pump performance curves as a function of the oscillation amplitude r_{osc}.

In the following two Sections, the simulation model is described in general. The hydraulic part is described in more detail, as it is relevant for the experimental part of this paper.

4.2 Actuator

The circulating eccentric oscillation needed to run the pump is efficiently generated by the oscillating armature motor. The dynamic vibration behavior of this novel actuator concept for operating peristaltic pumps means that the complete pumping system needs to be simulated. An MBS model [17] of the oscillating armature motor is being developed for

this purpose. The input to this model are the electromechanical transducer forces F, which are calculated with the help of a finite element analysis (FEA model) [17]. Thus, the MBS model can calculate the coupler oscillation amplitude r_{osc} as a function of the electromechanical transducer current.

4.3 Pumping principle

The basis for the hydraulic model of the pumping principle developed in this work is the electric-hydraulic analogy [18, 19]. The pump operation is simulated in this approach by means of a volume flow source Q_{disp}, a backflow branch and the resistor. Figure 11 shows the simplified hydraulic equivalent circuit. Q_{disp} is a controlled source that represents the periodically displaced volume resulting from the oscillation of the coupler. The elements R_i, L_i and C_i represent the branch of the backflow Q_{back} within the residual gap. In addition to the flow resistance R_i, the inertia of the flowing medium is represented by L_i and the compliance of the pump tube by C_i. The elements R_{res} and C_{res} are located at the pump output and represent the dynamic flow resistor. As a function of p_Q, the hydraulic resistance R_{res} and the associated hydraulic capacity C_{res} are used for decoupling the volume flow Q_{out} (see Section 2.5).

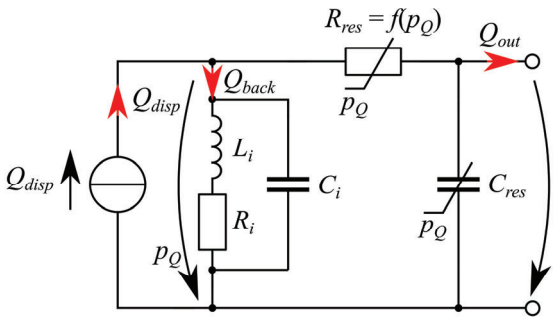

Fig. 11: Electric-hydraulic analogy to simulate the pump performance curves (according to [2]). The hydraulic model consists of the volume flow source Q_{disp}, the backflow branch with the elements L_i, R_i and C_i and the resistor which is represented with R_{res} and C_{res}.

The geometry of the coupler, the housing and the tube, the compliance of the tube, the oscillation amplitude r_{osc}, and the oscillation frequency f are central parameters in the hydraulic model, which is used to characterize the pump using pump performance curves. Finally, the model was developed and implemented using the SimulationX software package (version 3.8, ESI ITI GmbH) based on the mentioned parameters and the described electric-hydraulic analogy.

5 Experimental setup

The pump performance curves are acquired using the experimental setup depicted in Figure 12. A silicone tube (type: ECC-SIK, from Raumedic) [20] with an inner diameter $d_{tube,i}$ = 3/16" (≈ 4.8 mm) and a wall thickness w_{tube} = 1/16" (≈ 1.6 mm) is selected for the experiment. With this tube, the selected geometry of the pump section results in a residual gap w_{gap} = 3 mm for r_{osc} = 0. During pump operation, the residual gap w_{gap} decreases by the size of the selected oscillation amplitude r_{osc}. The simulation model is initially validated with water (H_20) as process liquid. The coupler oscillation amplitude r_{osc} is measured during pump operation by two optical distance sensors. The hydraulic parameters flow Q_{out} and back pressure p_{out} are respectively measured by a flow sensor and a pressure sensor integrated in the circuit. The back pressure is generated by an adjustable throttle valve.

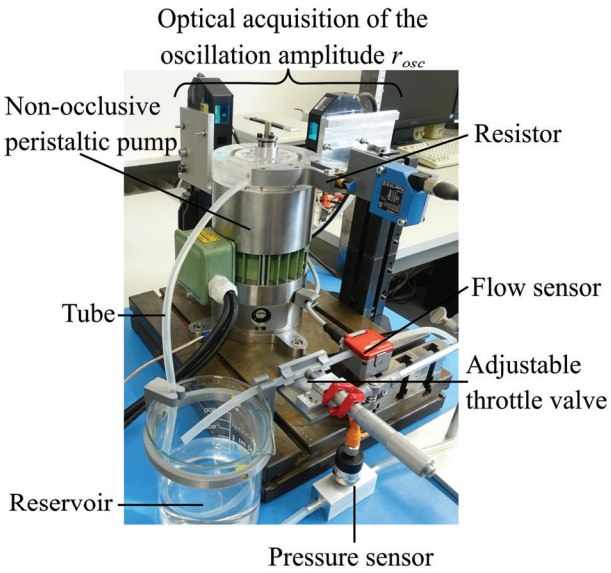

Fig. 12: Experimental setup (according to [2]) for acquiring the pump performance curves by measuring the back pressure p_{out} and the flow Q_{out} at the pump outlet as a function of the oscillation amplitude r_{osc}.

6 Results

6.1 Experiment: hydraulic model validation

The pressure-volume flow characteristic curve (pump performance curve) is the most important hydraulic pump characteristic. Hence, the hydraulic model of the non-occlusive peristaltic pump is validated by a pump performance curve with typical operating parameters (r_{osc} = 200 µm, f = 100 Hz). Tests show that during pump operation the coupler oscillation amplitude varies around the set mean value $r_{osc,a}$ = 200 µm within a complete cycle φ = (0 ... 360)°. A minimum amplitude $r_{osc,l}$ = 163 µm and a maximum amplitude $r_{osc,u}$ = 232 µm were found to occur. Asymmetries in the pump design, which result in an elliptical coupler trajectory, are the reasons for these tolerances.

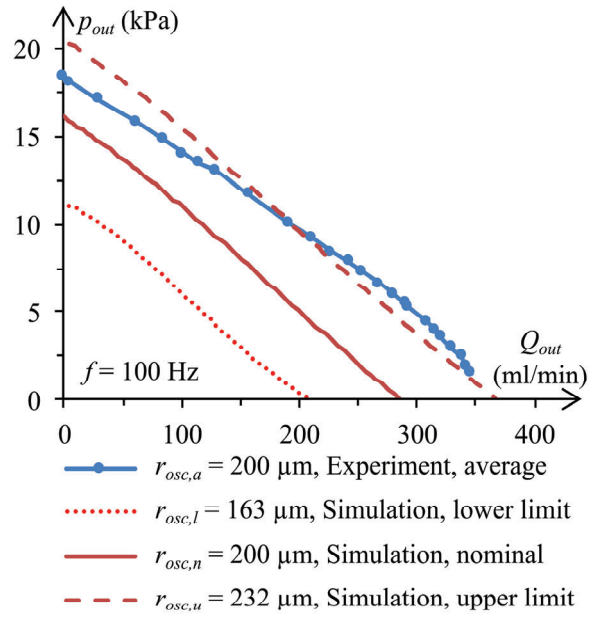

Fig. 13: Pump performance curves for hydraulic simulation model validation with an oscillation frequency f = 100 Hz. The measured curve (blue) with an average oscillation amplitude r_{osc} = 200 µm fits the simulated curve for $r_{osc,u}$ = 232 µm (red, dashed graph).

The blue curve in Figure 13 represents the measured pump performance curve for $r_{osc,a}$ = 200 µm and f = 100 Hz. Performance curves of the upper ($r_{osc,u}$, red dashed graph) and lower ($r_{osc,l}$, red dotted graph) tolerance limits are plotted next to the simulated nominal value curve ($r_{osc,n}$, red graph) to cater for the oscillation amplitude r_{osc} tolerance, as described above.
The graphs show that the measured characteristic curve $r_{osc,a}$ has larger pressures and flows than the nominal value curve $r_{osc,n}$ from the simulation model. This trend corresponds to a shift of the performance curves in the direction of both coordinate axes and is based on the tolerance range of the oscillation amplitude r_{osc}. Furthermore, it is evident that the measured pump characteristic curve $r_{osc,a}$ deviates only slightly from the simulated curve with $r_{osc,u}$. This is caused by the volume flow Q_{disp} generated by displacement resulting from the eccentric oscillation of the coupler. The local increase in the oscillation amplitude to $r_{osc,u}$ during the eccentric oscillation of the coupler causes a rise of Q_{disp} and leads to an increase in the flow Q_{out} and the pressure p_{out} at the pump output. The counteracting locally occurring minimum oscillation amplitude $r_{osc,l}$ cannot offset the increase in Q_{disp} because of the pump tube inertia.
Another reason for the deviation between measured and simulated pump curve can be found in the hydraulic model. Due to the modelling with the approach of the electric-hydraulic analogy, the hydraulic model can only represent the real prevailing effects to a limited extent. This includes the propagation of the pulse wave within the pump tube, which cannot be represented in the model. This limitation of the model contributes to the shifted simulated pump performance curve $r_{osc,n}$ in relation to the measured pump performance curve $r_{osc,a}$.

6.2 Experiment: pump characteristics

Figure 14 shows the measured performance curve field of the non-occlusive peristaltic pump as a function of the oscillation amplitude r_{osc}. The curves were recorded with an oscillation frequency of f = 100 Hz.

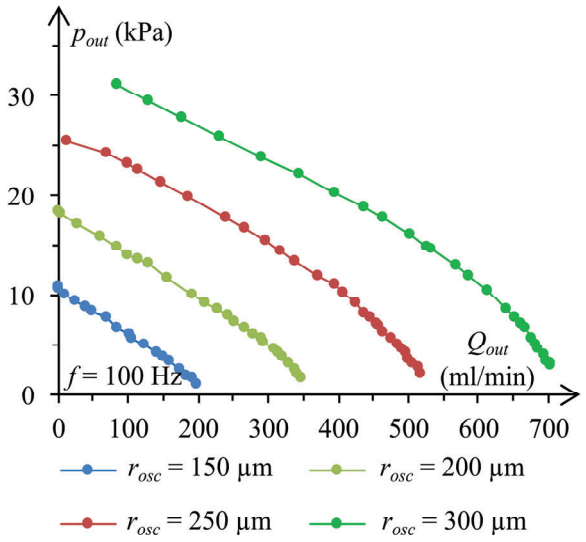

Fig. 14: Experimental performance curves of the non-occlusive pump as a function of the oscillation amplitude r_{osc} with an oscillation frequency f = 100 Hz.

The measured performance curves show that an increase in r_{osc} results in a uniform displacement of the pump performance curve in the direction of both coordinate axes. Furthermore, this displacement is independent of the slope of the pump curve, which corresponds to the effective internal hydraulic resistance of the pump. This characteristic shows the excellent controllability of the pump performance by adjusting the oscillation amplitude r_{osc}.

6.3 Experiment: red blood cell damage

The red blood cell damage caused by the non-occlusive peristaltic pump was investigated in direct comparison with a conventional roller pump (Ismatec, Pro-280 ISM 785) in an initial experiment with pig's blood and two identical circuits (reference circuit and test circuit). Figure 15 shows the experimental setup with the two identical blood circuits

except for the pumps. Each of them consists of pump, oxygenator, reservoir and peripherals with heat exchanger and gas supply.

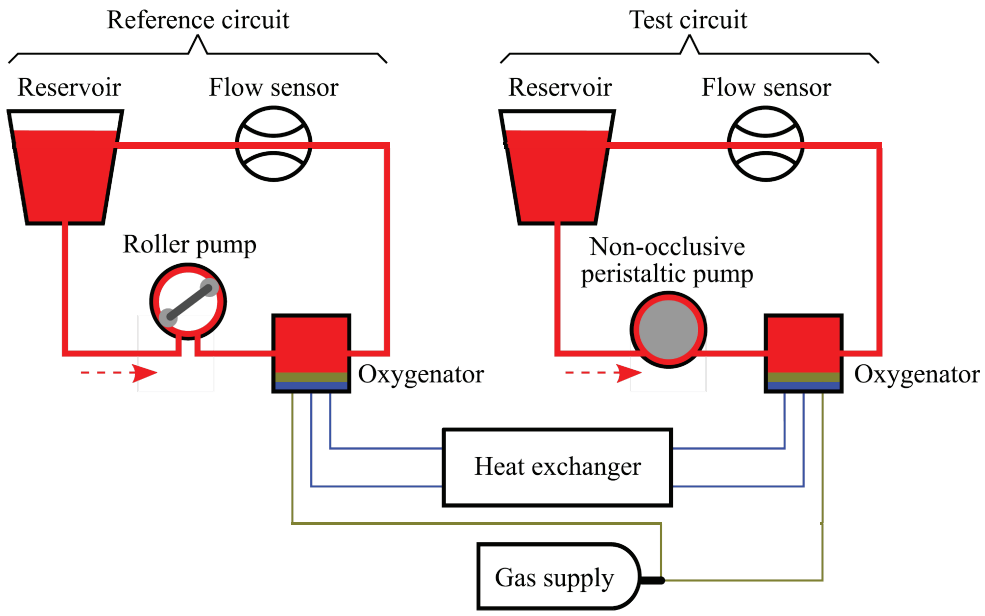

Fig. 15: Schematic illustration of the blood circuits to compare the red blood cell damage. We use a conventional roller pump in the reference circuit on the left side and the non-occlusive peristaltic pump runs the test circuit on the right side.

Blood from the same sample was used in both circuits for the experiment. This ensures equal starting conditions for evaluating blood damage. The blood circulates for a duration of 240 min and a flow of Q = 300 ml/min in the circuits. An oscillation amplitude r_{osc}= 250 µm with f = 104 Hz was set for the non-occlusive peristaltic pump to adjust the flow rate. This results in a residual gap width w_{gap} = 2.75 mm. We determined free plasma hemoglobin *fHb* photometrically and measured total hemoglobin *Hb* within blood samples every 30 min. After 240 min the relative plasma hemoglobin fraction *fHb*/*Hb* of the reference circuit blood was 4.699±0.002 ‰ and of the test circuit blood 2.093±0.310 ‰. Thus, the blood damage in the test circuit was reduced by 55.5 % with respect to the reference circuit. This single experiment shows that the pump technology developed here causes significantly less hemolysis than conventional roller pumps.

7 Discussion

There is a conflict of goals with the approach to develop a pumping principle that avoids complete tube occlusion: The mechanical stress on the process fluid should be as low as possible with the hydraulic power delivered by the pump being as high as possible. This conflict is resolved by installing a resistor at the output of the non-occlusive pump. The resistor throttles the backflow and allows the displaced volume to pass through, triggered by the pulse wave that propagates through the pump tube.

The experiment with the pump performance curves shows that the hydraulic pump characteristics can be simulated with the described model. In our opinion, this validates the hydraulic simulation model and it is suitable for dimensioning pumps based on the non-occlusive principle as described.

The pump performance curve field captured in the experiment shows the excellent control characteristics of the pumping principle. This controllability feature also enables dynamic volume flow pulsation by modulating the oscillation amplitude r_{osc}. The pump technology could conceivably be used in this operating mode for generating flow pulses that imitate the human heartbeat.

We found significantly lower hemolysis than with a comparable conventional roller pump in our first hemolysis investigation. This demonstrates the potential of the presented non-occlusive pumping principle. The experimental results may vary if the experiment is repeated due to fluctuations in blood composition, blood quality and the pig's state of health. Therefore, a larger study needs to be conducted in future to validate the results regarding the red blood cell

damage caused by the pumping principle. Nevertheless, we believe that a confirmation of the experimental results can be expected due to the relatively large difference between the hemolysis of the conventional roller pump and the non-occlusive peristaltic pump.

8 Conclusion

The pumping principle presented in this paper allows pump operation without complete tube occlusion. Optimization calculations can be conducted with our simulation models. For example, the pump section geometry could be modified as well as the design of the oscillating armature motor or the resistor. In this context, hydraulic parameters such as maximum back pressure or the scaling of the pump design can be typical optimization targets. This would allow the pumping principle to be specified for a specific application such as extracorporeal blood circulation, dialysis or organ perfusion systems.

The aforementioned limitation of the maximum application duration of today's extracorporeal blood circulation systems can be breached by reducing the blood damage – as caused by conventional roller pumps – with our new and innovative pumping principle.

Bibliography

[1] M. Quante and S. G. Tullius. Konservierungsmethoden von Organen für die Transplantation. *Deutsches Ärzteblatt*, 112(6):235-237, 2015.

[2] S. Pech. *Nicht-okklusive Schlauchpumpe zum schonenden Transport von sensiblen Medien*. PhD-Thesis, Technische Universität Dresden, Fortschritt-Berichte VDI, 17(298), VDI Verlag, Düsseldorf, ISBN: 978-3-18-329817-4, 2020.

[3] D. Arora, M. Behr and M. Pasquali. Blood damage measures for ventricular assist device modelling. *Moving Boundaries VII-Computational Modelling of Free and Moving Boundary Problems*, pp. 129-138, 2003.

[4] H.-D. Polaschegg. Red Blood Cell Damage from Extracorporeal Circulation in Hemodialysis. *Seminars in Dialysis*, 22(5):524-531, 2009.

[5] J. W. Mulholland, J. C. Shelton and X. Y. Luo. Blood flow and damage by roller pumps during cardiopulmonary bypass. *Journal of Fluids and Structures*, 20(1):129-140, 2005.

[6] L. B. Leverett , J. D. Hellums, C. P. Alfrey and H. C. Lynch. Red Blood Cell Damage by Shear Stress. *Biophysical Journal*, 12(3):257-273, 1972.

[7] C. Schmid and A. Philipp. *Leitfaden extrakorporale Zirkulation*. Springer Medizin Verlag, Heidelberg, 2011.

[8] R. Paul, J. Apel, S. Klaus, F. Schügner, P. Schwindke and H. Reul. Shear Stress Related Blood Damage in Laminar Couette Flow. *Artificial Organs*, 27(6):517-529, 2003.

[9] G. P. Noon, L. E. Kane, L. Feldman, J. A. Peterson and M. E. DeBakey. Reduction of Blood Trauma in Roller Pumps for Long-Term Perfusion. *World Journal of Surgery*, 9(1):68-71, 1985.

[10] M. Bluestein and L. F. Mockros. Hemolytic Effects of Energy Dissipation in Flowing Blood. *Medical and Biological Engineering*, 7(1):1-16, 1969.

[11] B. K. Kusserow and L. W. Kendall. In Vitro Changes in the Corpuscular Elements of Blood Flowing in Tubular Conduits. *ASAIO Journal*, 9(1):262-268, 1963.

[12] G. E. William, S. Attar, B. Baker, J. Chyba, A. D. Demetriades and R. A. Cowley. An Improved 360° Single Roller Spring Loaded Blood Pump. *ASAIO Journal*, 7(1);167-174, 1961.

[13] D. J. Rwan, H. K. Harris, J. B. Riley, D. N. Yoda and M. M. Blackwell. An under-occluded roller pump is less hemolytic than a centrifugal pump. *Journal of Extracorporeal Technology*, 29(1):15-18, 1997.

[14] S. Pech, H. Rathmann and R. Richter. Dresden University of Technology. Elektrisch betreibbare Schlauchpumpe. Disclosure patent, DE 10 2017 114 950 A1 (05.07.2017).

[15] S. Pech, H. Rathmann, R. Richter and J. Lienig. Electromagnetic Actuator of a Gentle Pump Mechanism for Blood Transport. Proceedings of the 59th Ilmenau Scientific Colloquium (59th IWK),11-15.09.2017, Ilmenau, Germany, 2017.

[16] S. Pech, H. Rathmann and R. Richter. Dresden University of Technology. Schlauchpumpe. Disclosure patent, DE 10 2019 102 432 A1 (31.01.2019).

[17] S. Pech, H. Rathmann, R. Richter and J. Lienig. Multibody Simulation of an Electromagnetic Actuator for a Gentle Blood Pump Mechanism. Proceedings of the 4th World Congress on Electrical Engineering and Computer Systems and Science (EECSS'18), 21-23.08.2018, Madrid, Spain, 2018.

[18] A. S. Dannenberg. *Einweg-Mikro-Membranpumpen mit trennbarer Aktorik zur Insulindosierung*. PhD-Thesis, Albert-Ludwigs-Universität Freiburg im Breisgau, 2016.

[19] H.-W. Grollius. *Grundlagen der Hydraulik*. 7. Aufl., Carl Hanser Verlag, München, 2015.

[20] Raumedic AG, ECC-Schlauch, https://www.raumedic.com/de/ technologien/extrusion/ecc-schlauch/, cited: 25.05.2021, 2021.